the fluid permeation. The effect is basically due to the flow of fluid that has permeated the membrane.

Nomenclature

A_s	=	wetted hole area of supporting plate	[mm^2]
D_s	=	thickness of supporting plate	[mm]
d	=	nominal pore size of membrane	[μm]
d_M	=	maximum pore size of membrane	[μm]
d_m	=	equivalent pore size of membrane	[μm]
k_A	=	permeability coefficient of air	[m^2]
k_L	=	permeability coefficient of liquid	[m^2]
k_T	=	substantial permeability coefficient	[m^2]
L	=	membrane thickness	[μm]
L_S	=	wetted hole perimeter of supporting plate	[m]
N	=	pore number of supporting plate	[—]
P_S	=	spreading pressure	[N/m]
ΔP	=	pressure difference across membrane	[kPa]
Q	=	permeation rate	[m/s]
Q_O	=	excess or deficient permeation rate	[m/s]
T	=	liquid temperature	[K]
γ_L	=	liquid surface tension	[N/m]
γ_S	=	solid surface tension	[N/m]
γ_{LS}	=	solid-liquid interfacial tension	[N/m]
ε_m	=	membrane porosity	[—]
ε_S	=	porosity of supporting plate	[—]
η	=	viscosity	[Pa·s]
θ	=	contact angle of liquid	[rad]
ϕ	=	interaction parameter defined by Eq. (4)	[—]
ψ	=	angle of inclination of membrane unit	[rad]

Literature Cited

1) Fox, H. W. and W. A. Zisman: *J. Colloid Sci.*, **7**, 109 (1950).
2) Fowkes, F. M.: *J. Phys. Chem.*, **66**, 1863 (1962).
3) Tamura, S.: *Kagaku-Zoukan*, p. 177 (1978).
4) Ueyama, K., S. Kittaka and S. Furusaki: *Kagaku Kougaku Ronbunshu*, **10**, 775 (1984).
5) Unno, H. and I. Inoue: *Kagaku Kougaku Ronbunshu*, **2**, 360 (1976).
6) Unno, H., H. Saka and T. Akehata: *J. Chem. Eng. Japan*, **19**, 281 (1986).

TURBULENT AND BROWNIAN DIFFUSIVE DEPOSITION OF AEROSOL PARTICLES ONTO A ROUGH WALL

MANABU SHIMADA, KIKUO OKUYAMA, YASUO KOUSAKA AND KENTARO OHSHIMA

Department of Chemical Engineering, University of Osaka Prefecture, Sakai 591

Key Words: Aerosol, Brownian Diffusion, Particle Deposition, Rough Wall, Turbulent Diffusion

The diffusive deposition of aerosol particles onto a rough wall in a turbulent flow field has been experimentally studied, using a stirred tank having a sand-roughened inside wall and uncharged monodisperse particles of 0.01–0.2 μm diameter. The experimental results showed that the deposition rate of particles onto the rough surface is enhanced, as the roughness increases, compared with that onto a smooth surface. The enhancement depends upon size of particles, intensity of turbulence and roughness of the wall, and is found to be significant when particle size and turbulent intensity are large. To explain the mechanism of the deposition, a model in which the existence of a particle-free layer above the bottom of the roughened wall is assumed is presented. The enhancement of the deposition obtained in the experiments can be described well by this model, and the enhancement results mainly from turbulent diffusion near the wall.

Introduction

Particles suspended in a gas stream are transported onto solid surfaces by diffusion, gravity, inertia and external forces. The mechanisms of particle deposition depend complicatedly on physical and electrical properties of the particles and the flow of the fluid in which the particles are suspended. Moreover, when the walls on which particles deposit are not smooth, surface roughness influences the process of deposition.

In this work, deposition of aerosol particles due to turbulent and Brownian diffusion from a stirred, turbulent fluid onto sand-roughened walls was experimentally studied. Surface contamination of silicon wafers during the manufacture of semiconductor devices is an example of particle deposition onto rough surfaces. In the field of dry deposition of atmospheric

Received April 24, 1986. Correspondence concerning this article should be addressed to M. Shimada.

aerosols, the ground surface of the earth is taken to be rough because of vegetation or terrain.

Chamberlain's experiment[2] is well known as an attempt to investigate particle deposition onto rough surfaces. Yaglom and Kader[16] theoretically derived equations for heat and mass transfer toward rough walls inside a pipe. Hahn *et al.*[10] made deposition experiments of particles onto a rough surface having repeated ridge-like protrusions, and compared their results with the theory of Kader and Yaglom.[11] The scale of wall roughness investigated in these studies was very much larger than the scale of sand roughness. The experimental results of Wells and Chamberlain[15] have been often cited in studies involving a smaller scale of roughness. In their experiments, filter papers with fibrous protrusions were used as the rough surface, and the deposition rate of particles of 0.65–5 μm in diameter was measured. Fernandez de la Mora and Friedlander,[5] and Gutfinger and Friedlander[9] proposed theories which took both free flight of particles and collection efficiency of fibers into account. A theoretical evaluation of particle deposition onto walls having irregularly shaped sand-type roughness, also based on a free-flight model, was proposed by Browne[1] and by El-Shobokshy and Ismail.[4] So far, no study has dealt with the deposition rate of particles by turbulent and Brownian diffusion onto walls having sand-type roughness.

The purpose of this paper is to clarify the influences of wall roughness of sand type upon the deposition of particles due to turbulent and Brownian diffusion. Uncharged monodisperse particles of 0.01–0.2 μm diameter are used, and wall loss of particles inside a stirred tank is measured in the experiment. Deposition rates of particles experimentally obtained are compared with those obtained with smooth walls, and the influences of the wall roughness on particle deposition are discussed. Then a model to explain the process of particle deposition onto a rough wall is proposed.

1. Experimental Apparatus and Method

Figure 1 shows a schematic diagram of the experimental apparatus, which is the same as that used in deposition experiments in a stirred tank having a smooth surface.[14] The vessel used is made of acrylic resin and is equipped with four vertical baffles. The total inner surface area S_T and the volume of stirred tank V_T are 0.12343 m^2 and 2.6060×10^{-3} m^3, respectively. A six-bladed turbine impeller and a three-bladed propeller are used as stirrers.

To make the walls rough, four kinds of sandpapers were fixed on the inner surfaces of the tank. **Figures 2**(a)–(d) are electron micrographs of the surface of the sandpapers used. Densely packed roughness elements

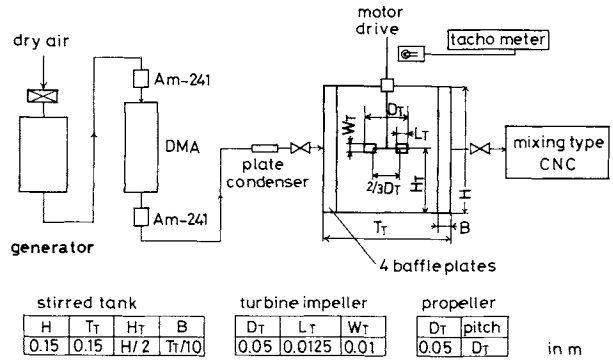

Fig. 1. Schematic diagram of experimental apparatus.

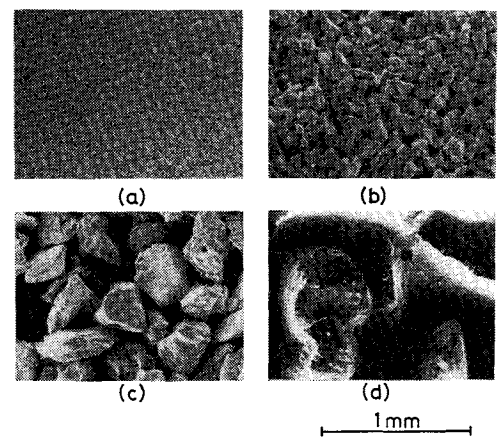

Fig. 2. Micrographs of surface of each sandpaper. Average height of roughness: (a), 11.2 μm; (b), 29.2 μm; (c), 119.2 μm; (d), 204.8 μm.

(abrasives) are seen on each surface of the sandpaper, forming a powder layer. The surface roughness was measured by a roughness gauge based on a tracing stylus method. That is, the surface of each sandpaper was traced with a tip of a tapered stylus, and the displacements of the stylus normal to the sandpaper were recorded. **Figure 3** shows examples of the distributions of roughness heights of sandpapers (b) and (c). The average heights of the roughness $2y_{rms}$ were defined as the double of root-mean-square of the displacements from the mean values, and they were obtained as 11.2, 29.2, 119.2 and 204.8 μm, for sandpapers (a), (b), (c) and (d) in Fig. 2, respectively.

The aerosol particles used were uncharged monodisperse NaCl and diethylhexylsebacate (DEHS) with diameters between 0.01 μm and 0.18 μm[14]. NaCl particles are solid and DEHS particles are liquid.

An aerosol was introduced throughout the tank and was stirred at a constant stirrer speed for a certain period to make the aerosol sufficiently uniform. Then a part of the outlet aerosol was sampled and introduced into a mixing-type condensation nuclei counter (CNC)[13] to count the initial number concentration of particles. After the sampling, the tank was confined and the aerosol was stirred at a given

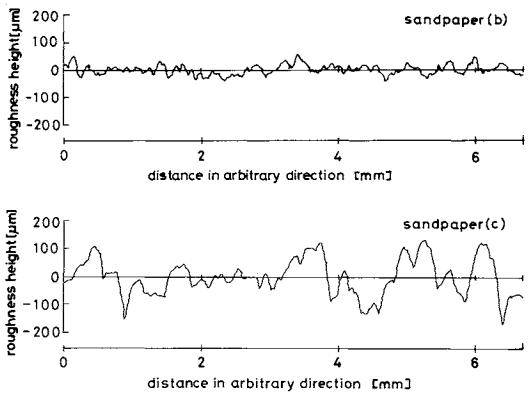

Fig. 3. Height distribution of surface roughness of sandpapers (b) and (c).

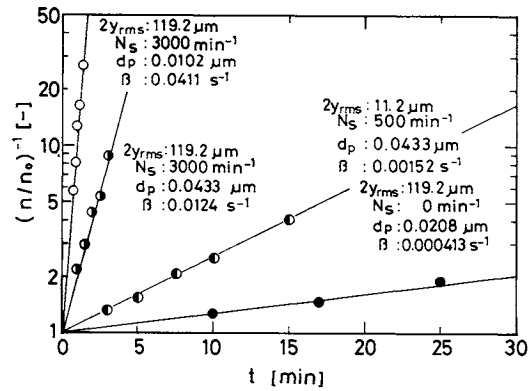

Fig. 4. Change in particle number concentration with stirring time.

stirrer speed. The range of stirrer speed was between 300 and 3000 r.p.m. The stirrer speed was monitored by a photo transistor during the experiment. The aerosol for any given residence time was sampled again, and its particle number concentration was also measured by the CNC. The decrease in particle number concentrations with time was observed for various experimental conditions.

2. Experimental Results and Discussion

2.1 Experimental results

The decrease in particle number concentrations in a system without coagulation of particles can be expressed as[7,14]

$$n = n_0 \exp(-\beta t) \tag{1}$$

where t is the stirring time, n_0 is the initial particle number concentration, and β is the deposition rate constant. **Figure 4** shows typical experimental results on changes in particle number concentrations inside the stirred tank having rough walls. It is seen that the concentrations tend to decrease linearly and thus Eq. (1) holds. Deposition rate constant β is given by the slope of the lines in the figure.

Figures 5(a)–(d) show the value of the deposition rate constant β experimentally obtained with the six-bladed impeller at various conditions. It is seen that there is no difference between NaCl and DEHS particles. Since the main mechanisms of particle deposition are turbulent and Brownian diffusion, the values of β increase with decreasing particle diameter due to Brownian diffusion. The values of β also increase with the stirring speed; this is caused by turbulent diffusion. Dependence of β upon the roughness becomes significant as particle diameter and stirring speed increase.

2.2 Comparison of experimental results with the deposition theory for smooth surface

The particle transport flux in a steady state, $N(\theta)$, is usually expressed as[6]

$$N(\theta) = (D + D_E)dn/dy - nv_t \cos\theta \tag{2}$$

where y is the distance from the surface, D and D_E are Brownian and turbulent diffusion coefficients, respectively, v_t the terminal settling velocity of a particle, and θ the angle from y direction to gravity direction.

When a turbulent boundary layer is formed above the surface, the boundary condition of Eq. (2) is given as

$$\begin{aligned} n &= 0 \quad \text{at} \quad y = 0 \\ n &= n_c \quad \text{at} \quad y = \delta \end{aligned} \tag{3}$$

where n_c is the particle number concentration in the turbulent core.

Crump and Seinfeld[3] solved Eq. (2) with Eq. (3), approximating D_E to $K_e y^m$, and obtained the deposition velocity of particles, $K_s(\theta)$, as

$$\begin{aligned} K_s(\theta) &= N(\theta)/n_c \\ &= v_t \cos\theta / [\exp\{\pi v_t \cos\theta / \\ &\quad (m \sin(\pi/m) \sqrt[m]{K_e D^{m-1}})\} - 1] \end{aligned} \tag{4}$$

The deposition rate constant for a smooth surface, β_s, can be expressed in terms of $K_s(\theta)$ as follows[14].

$$\begin{aligned} \beta_s = \{&K_s(0)S_T(0) + K_s(\pi/2)S_T(\pi/2) \\ &+ K_s(\pi)S_T(\pi)\}/V_T \end{aligned} \tag{5}$$

From a deposition experiment onto smooth walls using the same stirred tank used in this study, K_e and m in Eq. (4) were obtained as [14]

$$K_e \approx 7.5\sqrt{2\varepsilon_0/15\nu}, \quad m \approx 2.7 \tag{6}$$

where ε_0 is the average energy dissipation rate per unit mass of a fluid and is given by[12]

$$\varepsilon_0 = (4/\pi)N_p(N_s^3 D_T^5 / T_T^2 H) \tag{7}$$

where N_p is power number.[12]

The solid lines in Figs. 5(a)–(d) are the calculated results of Eqs. (4) and (5). The deviations between the experimental results and the solid lines are considered

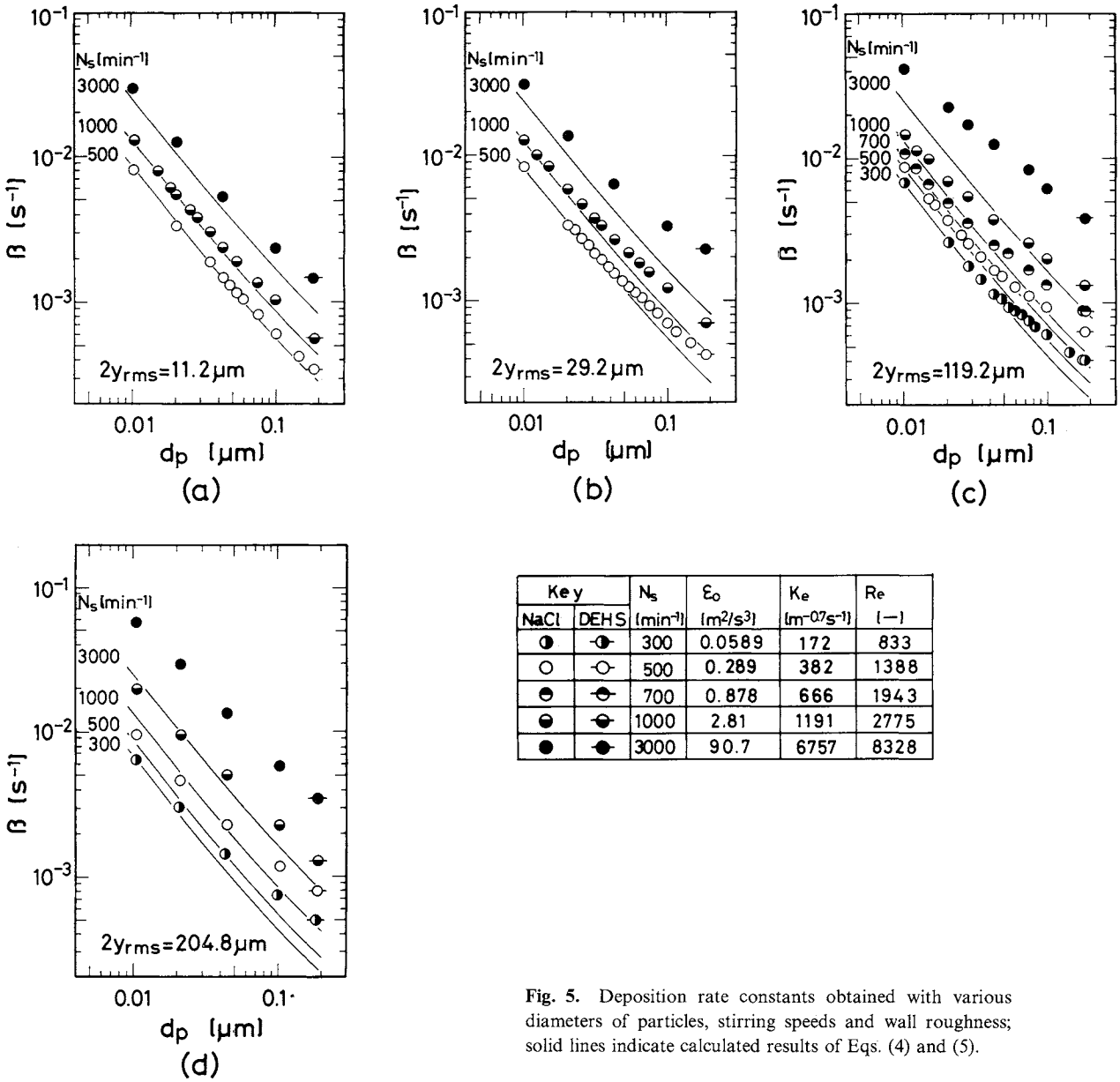

Key		N_s	ε_0	K_e	Re
NaCl	DEHS	(min^{-1})	(m^2/s^3)	$(m^{-0.7}s^{-1})$	(—)
◑	-◑-	300	0.0589	172	833
○	-○-	500	0.289	382	1388
◒	-◒-	700	0.878	666	1943
◒	-◒-	1000	2.81	1191	2775
●	-●-	3000	90.7	6757	8328

Fig. 5. Deposition rate constants obtained with various diameters of particles, stirring speeds and wall roughness; solid lines indicate calculated results of Eqs. (4) and (5).

to be due to the influence of wall roughness upon particle deposition, changes in volume and surface area of the stirred tank, and change in the energy dissipation rate inside the tank.

The change in volume of the tank due to the sandpapers is only a few percent of the total volume, so that this influence can be neglected. In regard to the surface area, the actual inner surface area of the tank is ten to one hundred times that of the tank with smooth surface because of unevenness. However, it is seen from Figs. 5(a)–(d) that the values of β obtained from the experiment are almost the same as those of β_s calculated from Eqs. (4) and (5) when the values of d_p and N_s are small. This agreement suggests that the actual increase of surface area has no direct effect on the deposition rate of particles.

In Eq. (7), if the value of ε_0 were altered due to the wall roughness, the values of β would deviate from the solid lines to almost the same degree for the entire range of particle size in Figs. 5(a)–(d). But it is seen from the figures that most of the experimental results agree closely with the solid lines when the size of particles is very small. Therefore, the change in the energy dissipation rate is thought to be small. Consequently, it is considered that the deviations between the experimental results and the solid lines in Figs. 5(a)–(d) are mainly due to the influence of the wall roughness upon the particle deposition.

From the Figs. 5(a)–(d), the values of β are found to be enhanced significantly with increasing values of d_p and N_s. It follows that the influence of roughness appears when the effect of turbulent diffusion becomes large or the effect of Brownian diffusion becomes small.

The results obtained with the three-bladed propeller as stirrer are shown in **Fig. 6**. There is no

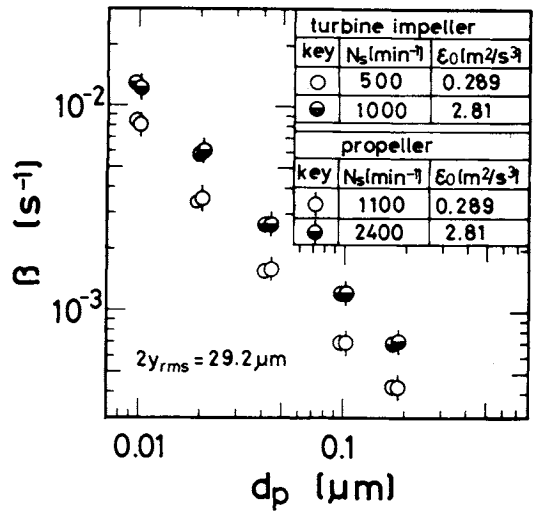

Fig. 6. Effect of type of stirrer on deposition rate.

difference between the two types of stirrer at the same values of ε_0. So it can be said that the intensity of the turbulence is represented by values of ε_0.

2.3 Model to describe the process of particle deposition onto a rough wall

When particles are transported to a rough wall, the particles are captured at the crests and the side wall of the roughness elements and thus cannot arrive at the bottom of the walls. **Figure 7** shows a concentration profile and a flow field used in the model proposed in this paper, in which the following conditions are assumed.

i) There exists a thin layer, h_f shown in Fig. 7, near the bottom of the rough surface where no fluid flows.[8] As a result, the longitudinal distribution of the turbulent diffusion coefficient shifts by the distance, h_f, from the bottom of the rough surface. That is,

$$D_E = K_e(y-h_f)^{2.7}. \tag{8}$$

ii) A particle transported toward the rough wall is captured by the roughened surface and cannot enter inside the distance, h_p, above the bottom of the turbulent boundary layer, h_f. This distance is designated as the "particle-free layer". There is no particle in the region $y \leqq h_p+h_f$.

Under the assumptions mentioned above, the basic equation of diffusion and the boundary conditions are given as follows.

$$\frac{d}{dy}\left\{(D+D_E)\frac{dn}{dy}\right\} - v_t\cos\theta\frac{dn}{dy}=0 \qquad h_p+h_f \leqq y \leqq \delta+h_f \tag{9}$$

$$\begin{aligned} n&=0 \quad \text{at} \quad y=h_p+h_f \\ n&=n_c \quad \text{at} \quad y=\delta+h_f \end{aligned} \tag{10}$$

Using $z=(y-h_f)\sqrt[2.7]{K_e/D}$ and $c=n/n_c$, Eq. (9) becomes

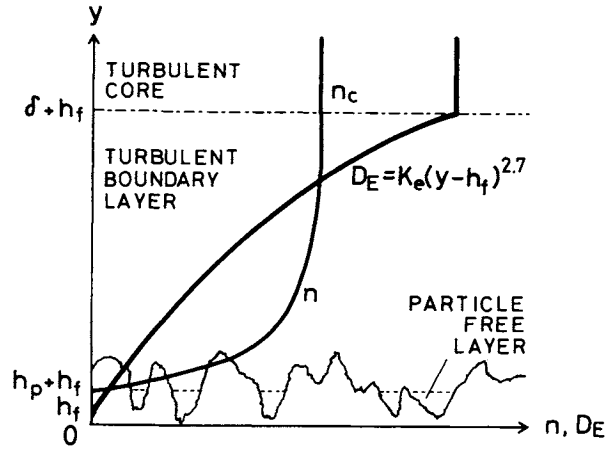

Fig. 7. Model for longitudinal distribution of particle number concentration and turbulent diffusion coefficient above rough surface.

$$\frac{d}{dz}\left[(1+z^{2.7})\frac{dc}{dz}\right] - \frac{v_t\cos\theta}{\sqrt[2.7]{K_eD^{1.7}}}\frac{dc}{dz}=0 \tag{11}$$

and Eq. (10) can be rewritten as follows.

$$\begin{aligned} c&=0 \quad \text{at} \quad z=h_p\sqrt[2.7]{K_e/D} \\ c&=1 \quad \text{at} \quad z=\delta\sqrt[2.7]{K_e/D} \end{aligned} \tag{12}$$

The analytical solution of Eqs. (11) and (12) is given by

$$c(z,\theta) = \frac{\exp[A\{\mathrm{Int}(z)-\mathrm{Int}(h_p\sqrt[2.7]{K_e/D})\}]-1}{\exp[A\{\mathrm{Int}(\delta\sqrt[2.7]{K_e/D})-\mathrm{Int}(h_p\sqrt[2.7]{K_e/D})\}]-1} \tag{13}$$

where

$$A = v_t\cos\theta/\sqrt[2.7]{K_eD^{1.7}} \tag{14}$$

and the functional form of Int is expressed as follows.

$$\begin{aligned} \mathrm{Int}(z) = -\frac{10}{27}\Bigg[&\log|z^{0.1}+1| \\ &+\sum_{i=1}^{13}\left\{\log\left|z^{0.2}-2z^{0.1}\cos\frac{(2i-1)\pi}{27}+1\right|\cos\frac{10(2i-1)\pi}{27}\right\} \\ &+2\sum_{i=1}^{13}\left\{\arctan\frac{\cos[(2i-1)\pi/27]-z^{0.1}}{\sin[(2i-1)\pi/27]}\sin\frac{10(2i-1)\pi}{27}\right\}\Bigg] \end{aligned} \tag{15}$$

The details of this calculation are shown in **Appendix**.

The value of Int(z) is nearly equal to 0.383 when z is much larger than unity. Since the Brownian diffusion coefficient, D, is much smaller than the turbulent diffusion coefficient at the upper end of the turbulent boundary layer, $D_E=K_e(\delta+h_f-h_f)^{2.7}$, it is admitted that $K_e\delta^{2.7}/D \gg 1$ and thus $\delta\sqrt[2.7]{K_e/D} \gg 1$. Accordingly, the deposition velocity onto a rough wall, $K_r(\theta)$, is calculated as

$$K_r(\theta)=\frac{1}{n_c}(D+D_E)\frac{dn}{dy}\bigg|_{y=h_p+h_f}$$
$$=(D+K_e h_p^{2.7})\sqrt[2.7]{K_e/D}\,\frac{dc}{dz}\bigg|_{z=h_p\sqrt[2.7]{K_e/D}}$$
$$=v_t\cos\theta/[\exp[A\{0.383-\mathrm{Int}(h_p\sqrt[2.7]{K_e/D})\}]-1] \tag{16}$$

and the deposition rate constant for rough walls, β_r, is given as follows.

$$\beta_r=\{K_r(0)S_T(0)+K_r(\pi/2)S_T(\pi/2)+K_r(\pi)S_T(\pi)\}/V_T \tag{17}$$

As the particle-free layer, h_p, becomes larger in the model, $K_r(\theta)$ in Eq. (16) increases. In such a case, it is seen from Fig. 7 that the y coordinate of the position where all the particles deposit becomes larger. Since the value of the turbulent diffusion coefficient increases with y, the contribution of turbulent diffusion near the particle-free layer is considered to become significant, resulting in the enhancement of deposition. On the other hand, when h_p is small, the effect of Brownian diffusion tends to dominate the particle deposition in the vicinity of the particle-free layer because D_E is small near the bottom of the wall. If $h_p=0$, $K_r(\theta)$ agrees with the deposition velocity onto a smooth wall, $K_s(\theta)$. Consequently, the influences of the roughness upon the deposition can be represented in terms of the values of h_p.

2.4 Dependence of particle-free layer on Brownian and turbulent diffusion and roughness height

Figures 8 and **9** show the values of h_p estimated from the values of β for sandpaper (c). Since the values of h_p cannot be derived analytically, the computation of h_p is made by trial and error by substituting the experimental values of β into Eqs. (16) and (17). To examine the dependence of the influence of roughness upon Brownian and turbulent diffusion, the abscissas of these figures are Brownian diffusion coefficient, D, and the inverse of the energy dissipation rate, ε_0^{-1}, respectively.

Larger values of h_p can be seen at smaller values of D (i.e. d_p is large) or ε_0^{-1} (i.e. N_s is large) in Figs. 8 and 9. This fact is considered as follows. Let us introduce the distance, $\bar{y}$, where the turbulent diffusion coefficient is equal to the Brownian diffusion coefficient. Setting $D_E=D$ in Eq. (8), $\bar{y}$ is given as follows.

$$\bar{y}=\sqrt[2.7]{D/K_e}+h_f \tag{18}$$

When the effect of turbulent diffusion becomes large compared with that of Brownian diffusion, the value of $\bar{y}$ in Eq. (18) tends to decrease. Then the turbulent diffusion coefficient, D_E, is not negligible in the vicinity of the particle-free layer compared with

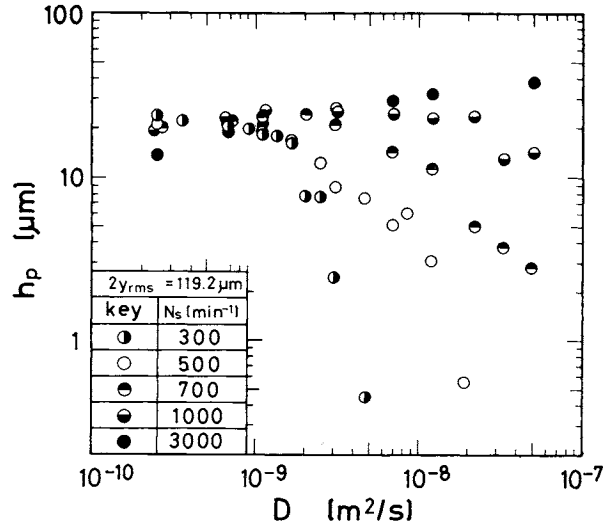

Fig. 8. Change in value of h_p for sandpaper (c) against Brownian diffusion coefficient, D.

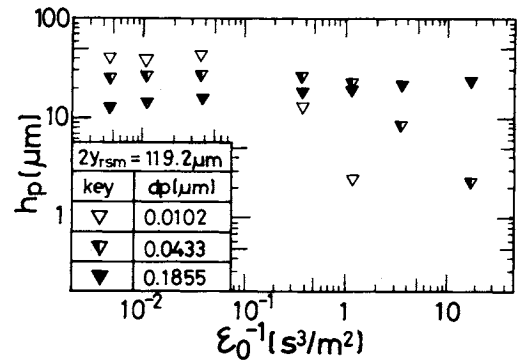

Fig. 9. Change in value of h_p against the inverse of energy dissipation rate, ε_0^{-1}.

the Brownian diffusion coefficient, D, as shown in **Fig. 10**(a). In such a case, the deposition flux toward the particle-free layer will be enhanced by the turbulent diffusion. Consequently, the influence of wall roughness becomes significant when D and ε_0^{-1} are small.

When the particle diameter and the stirring speed become small, the values of h_p in Figs. 8 and 9 become smaller. As the value of D increases or the turbulent intensity decreases, the value of $\bar{y}$ becomes gradually larger. This means that the relative effect of turbulent diffusion in the vicinity of the particle-free layer becomes smaller. Consequently, the enhancement of the deposition tends to decrease with the increase of D and ε_0^{-1}.

If the relative effect of turbulent diffusion becomes very small so that the hypothetical plane where $D_E=D$ rises to exceed the height of roughness sufficiently as shown in Fig. 10(b), Brownian diffusion comes to be predominant in the vicinity of the particle-free layer. In such a case, the deposition flux becomes almost equal to that on a smooth surface. As a result of this, the deposition rate of particles is

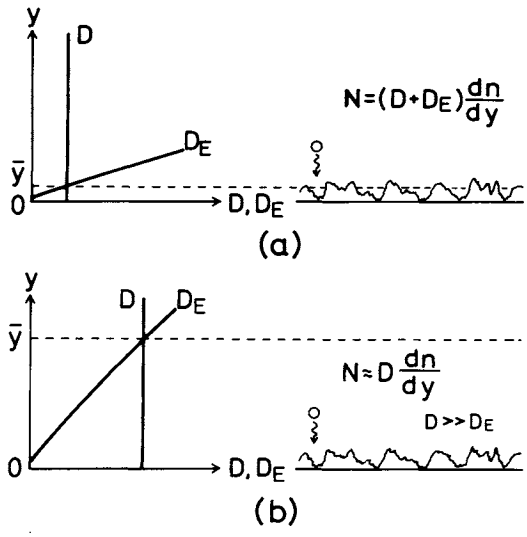

Fig. 10. Schematic illustration of particle deposition onto rough surface. (a), enhancement of deposition is significant; (b), enhancement of deposition is not significant.

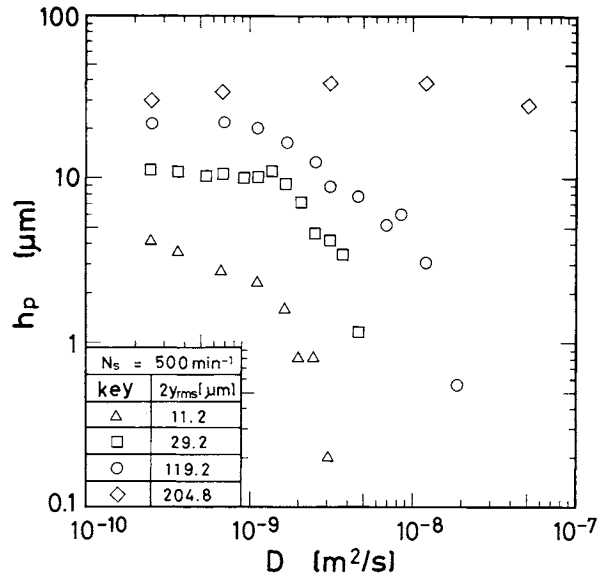

Fig. 11. Change in value of h_p against Brownian diffusion coefficient, D, for four kinds of sandpapers.

influenced very little by roughness. For example, when the stirring speed is 500 r.p.m. ($K_e=382$) and $D>2\times10^{-8}$ m^2/s, no influence of roughness is seen in Fig. 8. The value of $\bar{y}$ for this case is calculated from Eq. (18) as $\bar{y}>\sqrt[2.7]{2\times10^{-8}/382}\times10^6+h_f=(160+h_f)\,\mu$m. Thus the value of $\bar{y}$ is much larger than the average height of the roughness of sandpaper (c) ($2y_{rms}=119.2\,\mu$m). Therefore, no enhancement of deposition is seen.

Figure 11 shows the values of h_p for four kinds of sandpapers. The values of h_p for sandpaper (a) tend to decrease as D increases, and become zero near $D=4\times10^{-9}$ m^2/s. For sandpaper (d), the influence of roughness on h_p is seen to be almost constant even at large values of D. Generally, with increasing wall roughness the values of h_p tend to become large for given values of D and ε_0. When the wall roughness is small, the particle deposition can be described by Fig. 10(b). As the roughness becomes large, the particle deposition tends to be influenced by the turbulent diffusion as shown in Fig. 10(a), which causes the enhancement of deposition rate.

Conclusions

The Brownian and turbulent diffusive deposition of aerosol particles with diameters between 0.01 and 0.2 μm onto rough walls having an average height of roughness from 10 to 200 μm has been studied, and the following results were obtained.

(1) The deposition rate of particles onto rough walls is enhanced compared with that onto smooth walls. This enhancement is found to depend on size of particles, intensity of turbulence and roughness height. When the particle deposition is dominated by Brownian diffusion, the influence of roughness is found to be very small. As particle size and turbulent intensity become large, i.e. as turbulent diffusion increases, the enhancement of deposition rate comes to be significant. In this study, there exists a case in which the deposition rate increases to about four times that for a smooth wall.

(2) The rate of particle deposition onto rough walls has been derived by using a new model where the existence of a particle-free layer above the bottom of the rough wall is assumed. A method to estimate the thickness of the particle-free layer, h_p, is presented, and the estimated value of h_p from the experimental result is found to be large when particle size, turbulent intensity and roughness height are large. By calculating the relative contribution of Brownian and turbulent diffusion to the particle deposition in the vicinity of the wall, it is concluded that the enhancement of particle deposition is caused by turbulent diffusion near the particle-free layer.

Appendix

Setting $A=v_t\cos\theta/\sqrt[2.7]{K_eD^{1.7}}$ (Eq. (14)) and integrating Eq. (11) twice, we obtain

$$\int\frac{dc}{Ac+C_1}=\int\frac{dz}{1+z^{2.7}}+C_2 \tag{A-1}$$

where C_1 and C_2 are constants. If Int (z) is defined as the first term of RHS of Eq. (A-1), Eq. (A-1) becomes

$$\frac{1}{A}\log|Ac+C_1|=\mathrm{Int}(z)+C_2 \tag{A-2}$$

Substitution of Eq. (12) into Eq. (A-2) gives the solution of Eq. (11) as Eq. (13).

To obtain a functional form of Int (z), we set $t=z^{0.1}$, giving

$$\mathrm{Int}(z)=\int\frac{dz}{1+z^{2.7}}=10\int\frac{t^9}{1+t^{27}}dt$$
$$=-\frac{10}{27}\left[\log|t+1|+\sum_{i=1}^{13}\left\{\log\left|t^2-2t\cos\frac{(2i-1)\pi}{27}+1\right|\cos\frac{10(2i-1)\pi}{27}\right\}+2\sum_{i=1}^{13}\left\{\arctan\frac{\cos[(2i-1)\pi/27]-t}{\sin[(2i-1)\pi/27]}\sin\frac{10(2i-1)\pi}{27}\right\}\right] \tag{A-3}$$

Then Eq. (15) is obtained by substituting $t=z^{0.1}$.

Acknowledgment

We wish to thank Dr. S. Endo, of the Institute of Physical and Chemical Research, who kindly helped us with measuring the roughness of sandpapers.

Nomenclature

A	=	value given in Eq. (14)	[—]
B	=	width of baffle plate	[m]
$c, c(z,\theta)$	=	dimensionless particle number concentration	[—]
D	=	Brownian diffusion coefficient	[$m^2 s^{-1}$]
D_E	=	turbulent diffusion coefficient	[$m^2 s^{-1}$]
D_T	=	diameter of stirrer	[m]
d_p	=	particle diameter	[m]
H	=	height of stirred tank	[m]
H_T	=	fitting up height of stirrer	[m]
h_f	=	thickness of layer where no fluid flows	[m]
h_p	=	thickness of particle-free layer	[m]
Int	=	function defined in Eq. (15)	[—]
K_e	=	value given in Eq. (6)	[$m^{-0.7} s^{-1}$]
$K_r(\theta)$	=	deposition velocity for rough wall having angle θ, Eq. (16)	[$m s^{-1}$]
$K_s(\theta)$	=	deposition velocity for smooth wall having angle θ, Eq. (4)	[$m s^{-1}$]
L_T	=	width of turbine impeller	[m]
m	=	value given in Eq. (6)	[—]
N_p	=	power number	[—]
N_s	=	stirring speed	[min^{-1}]
$N(\theta)$	=	transport flux of particles onto smooth wall having angle θ, Eq. (2)	[$m^{-2} s^{-1}$]
n	=	particle number concentration	[m^{-3}]
n_c	=	particle number concentration in turbulent core	[m^{-3}]
n_0	=	initial particle number concentration	[m^{-3}]
Re	=	Reynolds number	[—]
S_T	=	total inner surface area of stirred tank	[m^2]
$S_T(\theta)$	=	surface area of wall having angle θ	[m^2]
T_T	=	diameter of stirred tank	[m]
t	=	stirring time	[s], [min]
V_T	=	volume of stirred tank	[m^3]
v_t	=	gravitational settling velocity	[$m s^{-1}$]
W_T	=	length of turbine impeller	[m]
y	=	distance from surface	[m]
$\bar{y}$	=	value expressed in Eq. (17)	[m]
z	=	dimensionless distance from surface	[—]
$2y_{rms}$	=	average height of roughness	[m]
β	=	deposition rate coefficient	[s^{-1}]
β_r	=	deposition rate coefficient on rough surface, Eq. (17)	[s^{-1}]
β_s	=	deposition rate coefficient on smooth surface, Eq. (5)	[s^{-1}]
δ	=	thickness of turbulent boundary layer	[m]
ε_0	=	energy dissipation rate, Eq. (7)	[$m^2 s^{-3}$]
θ	=	angle from y direction to gravity direction	[rad]
ν	=	kinematic viscosity of gas	[$m^2 s^{-1}$]

〈Subscripts〉

r	=	rough surface
s	=	smooth surface

Literature Cited

1) Browne, L. W. B.: *Atmos. Environ.*, **8**, 801 (1974).
2) Chamberlain, A. C.: *Quart. J. R. Meteor. Soc.*, **94**, 318 (1968).
3) Crump, J. G. and J. H. Seinfeld: *J. Aerosol Sci.*, **12**, 405 (1981).
4) El-Shobokshy, M. S. and I. A. Ismail: *Atmos. Environ.*, **14**, 297 (1980).
5) Fernandez de la Mora, J. and S. K. Friedlander: *Int. J. Heat Mass Transfer*, **25**, 1725 (1982).
6) Friedlander, S. K.: "Smoke, Dust and Haze," Wiley, New York (1978).
7) Fuchs, N. A.: "The Mechanics of Aerosols," Pergamon, New York (1964).
8) Grass, A. J.: *J. Fluid Mech.*, **50**, 233 (1971).
9) Gutfinger, C. and Friedlander, S. K.: *Aerosol Sci. Technol.*, **4**, 1 (1985).
10) Hahn, L. A., J. J. Stukel, K. H. Leong and P. K. Hopke: *J. Aerosol Sci.*, **16**, 81 (1985).
11) Kader, B. A. and A. M. Yaglom: *Int. J. Heat Mass Transfer*, **20**, 345 (1977).
12) Kagaku Kogaku Binran, 4th ed., p. 1316, Maruzen, Tokyo (1978).
13) Kousaka, Y., T. Niida, K. Okuyama and H. Tanaka: *J. Aerosol Sci.*, **13**, 231 (1982).
14) Okuyama, K., Y. Kousaka, S. Yamamoto and T. Hosokawa: *J. Colloid Interface Sci.*, **110**, 214 (1986).
15) Wells, A. C. and A. C. Chamberlain: *Brit. J. Appl. Phys.*, **18**, 1793 (1967).
16) Yaglom, A. M. and B. A. Kader: *J. Fluid Mech.*, **62**, 601 (1974).